Environmental Management (2012) 50:405–417
DOI 10.1007/s00267-012-9885-7

The Vegetation Coverage Dynamic Coupling with Climatic Factors in Northeast China Transect

Qin Nie · Jianhua Xu · Minhe Ji · Lei Cao · Yang Yang · Yulian Hong

Received: 19 September 2011 / Accepted: 17 May 2012 / Published online: 22 June 2012

Abstract Based on SPOT-VGT images and meteorological data, this paper applied an integrated method to investigate the vegetation dynamic and its response to climate factors during 1998–2008 in Northeast China Transect, one of 15 ecological transects listed in the International Geosphere–Biosphere Programme. The main findings are as follows: (1) The NDVI time series presented nonlinear patterns that vary with timescales. The series fluctuated greatly at the smallest timescale (20 days), showing no salient trend, whereas a trend manifested itself more and more with the increase of time scale and finally stabilized at the 320-day scale. Little difference was found between vegetation types about the NDVI periodicity, as they occurred on either a 280-day or a 290-day cycle. (2) NDVI exhibited a significant correlation with temperature, precipitation, and sunshine hours. Overall, the correlation between NDVI and temperature was the highest, followed by precipitation, sunshine hours, and relative humidity. For different vegetation types, the correlations between NDVI and climate variables diversified, increasing from desert steppe to typical steppe, meadow steppe, and forest. (3) The periodicity of temperature and precipitation occurred in either a 280-day or 290-day cycle, which was approximately coincident with that of NDVI. This further supported the significant relationship between NDVI and these two climate factors. (4) At all the time scales under examination, NDVI and temperature and precipitation are significantly, positively correlated, especially at the 160-day scale, which can be regarded as the most suitable time scale for investigating the responses of vegetation dynamics to climate factors at most stations.

Keywords Vegetation coverage · NDVI · Climate factors · Correlation · Wavelet transform · Northeast China Transect

Q. Nie · J. Xu (✉) · M. Ji · L. Cao · Y. Yang · Y. Hong
The Research Center for East-West Cooperation in China, The Key Lab of GIScience of the Education Ministry PRC, East China Normal University, Shanghai 200062, China
e-mail: jhxu@geo.ecnu.edu.cn

Q. Nie
School of Environment and Planning, Liaocheng University, Liaocheng 252059, China

Introduction

The International Geosphere–Biosphere Programme (IGBP) terrestrial transects have been viewed as a popular way for large-scale global change research (Gao and Zhang 1997; Zhang and others 1997a), and proven successful in seeking solutions to many complex problems of large scale research (Koch and others 1995; Steffen 1995; Steffen and others 1999; Canadell and others 2002), such as vegetation coverage dynamics and its influential climate factors. A transect is usually a long and narrow region with a major ecological gradient that is sensitive to global change. In 1993, the Northeast China Transect (NECT) was chosen as one of the 15 IGBP ecological transects by Global Change and Terrestrial Ecosystems (GCTE). Located between 42–46°N and 112–130.5°E, the transect is regarded as a good representation of a mid-latitude semi-arid gradient in terrestrial ecosystem studies and has ever since drawn a great deal of attention from the ecological science community (Koch and others 1995; Zhang and others 1997a; Steffen and others 1999; Ni and Zhang 2000).

During the last 40 years, many studies have been conducted in the NECT to elucidate the relationships among environment, ecosystem and human beings. Trying to reveal vegetation patterns and understand the response to

climate factors is one of the central tasks (Ni and Wang 2004), on which much research has been carried out so far. Many such characteristics of vegetation patterns as distribution, floristic composition and plant functional types were described, and their relationships to such major environmental factors as topography, soil, climate and land use were explored (Zhang and others 1997a, b, 1998; Ni and others 1999; Ni and Zhang 2000; Chen and Wang 2000; Chen and others 2000). Within the background of the global change, the changes of geographical distribution, frequency and dominance pattern for 16 tree species were analyzed, and the spatial correlation of tree species along the forested part of the NECT from 1986 to 1994 was computed (Chen and others 2003). Nonetheless, such kinds of transect studies are very limited mainly due to the lack of sufficient temporal–spatial scales. Up to this date, a detailed study of vegetation dynamics using Normalized Difference Vegetation Index (NDVI) and climate-vegetation interaction at multiple time scales has not been systematically undertaken in the NECT. The time series of NDVI and climate factors are usually non-stationary, i.e., they present different frequency components, such as seasonal variations, long-term and short-term fluctuations. Therefore, it is necessary to study vegetation coverage dynamics and the climate-vegetation interaction at different time scales.

In most existing studies, long-term observations at local meteorological stations and remote sensing images have typically been used as the test datasets. An example of the latter is a SPOT product, which can provide the required time-series of satellite images for vegetation dynamics studies (Ni and Wang 2004). Among the surface parameters extracted from the remote sensing data, NDVI can be used to characterize vegetation coverage and growth, which is calculated as the formula NDVI = (NIR − RED)/(NIR + RED), where NIR and RED are the reflectance in the near-infrared and red electromagnetic spectra of objects on the earth surface, respectively. The near-infrared is sensitive to changes in vegetation cell wall structure and rigidity, and the red to chlorophyll content and activity. Therefore NDVI is closely related to vegetation cover, phytomass, leaf area index and net primary productivity and can reflect the vegetation cover information objectively over large spatial and temporal scales. It has become a de facto standard approach to the research of environmental science, ecology and agriculture (Asrar and others 1984; Diodato and Bellocchi 2008; Garty and others 2001; Giannico 2007; Jarlan and others 2008; Li and others 2005; Zhang and others 2006).

On the other hand, the derived NDVI data have been heavily linked to such environmental factors as precipitation and temperature, as they are usually considered having the biggest impact on the vegetation growth. Since NDVI time series have proven useful to reflect the change of vegetation coverage to a certain extent, the studies on the relationship between NDVI and climate factors are hardly limited to terrestrial transect analyses, but become a hot topic in a much larger context of ecological research (Fu and others 2007). Despite advances in the response of NDVI to regional climate factors, the understanding of the mechanism and extent of the climatic influence on NDVI is far from complete (Cao and others 2012). The interaction between temperature, radiation and water impose complex and varying limitations on vegetation activity. In particular, few studies could take the periodicity into consideration and compute the cycle of NDVI and major climate factors. This would support the relationship between NDVI and climate variability from a new perspective.

In addition, developing new methods to effectively analyze multi-temporal data is an important issue for the remote sensing community. During the past decades, various methods were developed to detect temporal patterns of vegetation from multi-temporal data (Yang and others 2012), including statistical approaches (Hall-Beyer 2003), time series analyses (Udelhoven and others 2009), and spectral-frequency techniques (Stockli and Vidale 2004). Among these methods, wavelet transform (WT) has proven quite useful in the study of multi-scale and non-stationary processes over finite spatial and temporal domains (Furon and others 2008). It has been widely used for such remote sensing applications as image registration (Fonseca and others 1998), spatial and spectral fusion (Zhou and others 1998), feature extraction (Simhadri and others 1998), speckle reduction (Horgan 1998), texture classification (Zhu and Yang 1998), improving endmember estimation (Li and Bruce 2004) and crop phenology detection (Galford and others 2008; Sakamoto and others 2005). Usually, WT is used as a multi-resolution analysis (MRA) method, i.e., the signal is studied at a coarse resolution to obtain an overall view of the signal and at incrementally finer resolutions to see increasingly finer details (Burke-Hubbard 1998).

The objective of this paper is to identify the multi-temporal patterns of vegetation dynamics and its response to climate factors in the NECT using a combination of several methods. WT was first employed as a multi-resolution method to reveal the periodicity and nonlinear pattern of NDVI, giving us an overall understanding of the vegetation dynamics at different time scales. Secondly, based on the results of a correlation analysis, WT was then used to reveal the periodicity in the climate variables in attempt to analyze the relationship between NDVI and relevant climate variables from a new perspective. In the final step, a wavelet regression analysis (Xu and others 2008) was applied to reveal the quantitative relationship between NDVI and climate variables at the most suitable time scales.

Study Area and Data

Study Area

NECT was identified as a mid-latitude transect for terrestrial ecosystem studies by GCTE in 1993. The transect runs approximately parallel to 43.5°N and ranges from 42°N to 46°N and from 112°E to 130.5°E (Fig. 1). Because it is parallel to the latitude line, the theoretical radiation is uniform within the transect. However, the moisture gradient from east to west is very steep, with precipitation varying from 600 to 1,000 mm at the east end, from 300 to 600 mm in the middle and from 100 to 300 mm at the west end (Gao and Zhang 1997). Due to the increase of precipitation from the west to the east, vegetation varies gradually from desert grasslands and typical steppes in the west to temperature conifer-broadleaf mixed forests, deciduous broadleaf forests, and shrubs in the east, with meadow grasslands and agricultural lands in the middle (Zhang and others 1997a; Wang and others 2001).

Climate Data

The climate data used in this study was from 20 selected meteorological stations along the NECT (Fig. 1), provided by China Meteorological Data Sharing Service System (CMDSSS, http://cdc.cma.gov.cn). It included 10-day mean temperature (0.1°C), 10-day mean precipitation (0.1 mm), 10-day average relative humidity (1 %) and 10-day sunshine hours (0.1 h), covering the study period of April 1998 to July 2008. The standards of the measurement instruments and data processing have been outlined in the CMDSSS. The 20 stations covered a large portion of NECT from east to west at different altitudes, representing the four major vegetation types, with 6 stations in forest, 5 stations in meadow steppe, 8 stations in typical steppe, and 1 station in desert steppe.

NDVI Data

In this research, a time series of 372 SPOT-VGT scenes was obtained, covering the period from April 1998 to July 2008. The SPOT-VGT images-based NDVI time series data for the NECT was obtained from the Image Processing and Filing Center of VITO Institute, Belgium, which has been improved by applying atmospheric correction, cloud removal, and bi-directional reflectance distribution function (BRDF) correction. Each 10-day NDVI data was synthesized using a revised Maximum Value Composites (MVC) method [i.e. Max ($NDVI_1$, $NDVI_2$… $NDVI_i$)], meaning that for each location, the pixel with the highest NDVI value during 10 consecutive days was selected for the synthetic image. The 10-day periods of synthetic

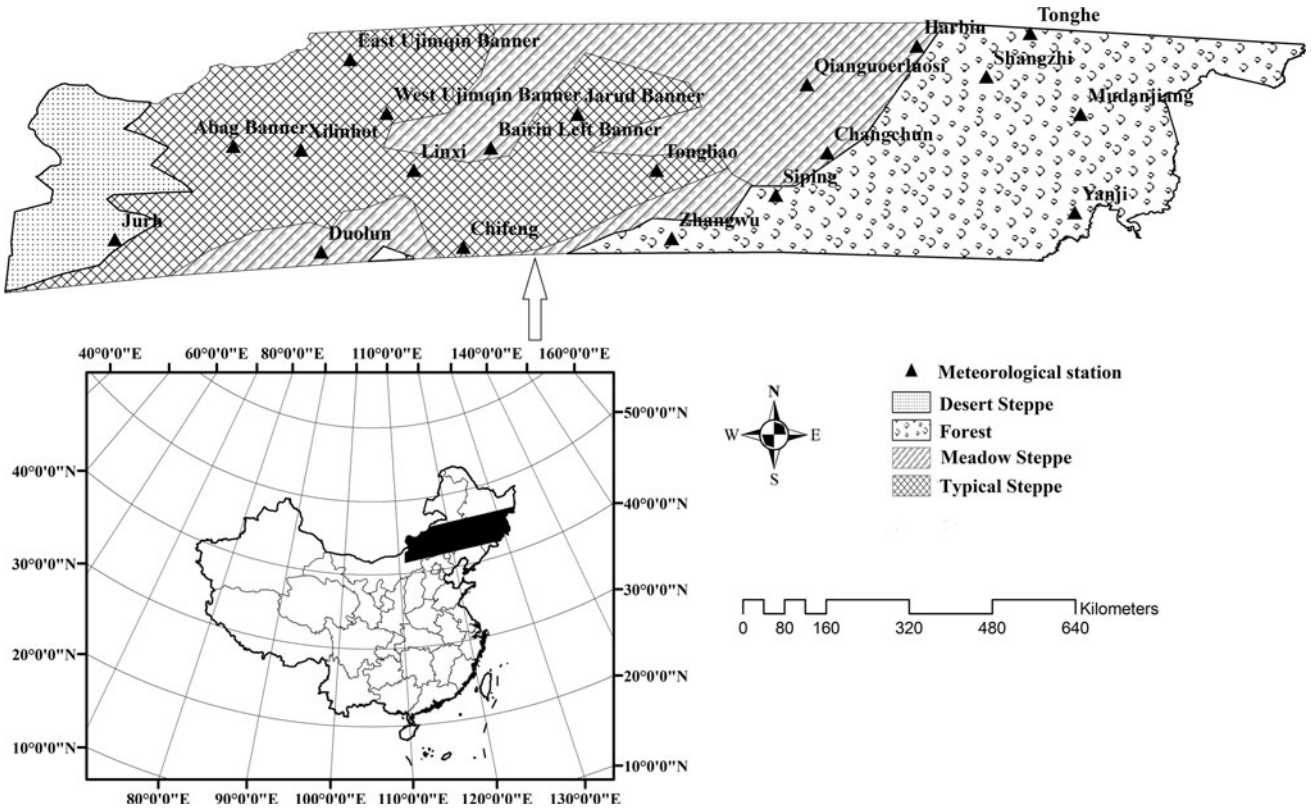

Fig. 1 Types of vegetation coverage and meteorological stations in the study area

SPOT-VGT scenes were defined as from date 1 to date 10, date 11 to date 20, and date 21 to the end of each month. The spatial resolution of the NDVI data was 1 × 1 km, nearly constant across the whole 2,250 km swath, which meant that there was almost no distortion at the image edge (Maisongrande and others 2004).

The SPOT-VGT images record the digital number (DN) between 0 and 255. For the convenience of display, the grey value of every pixel is linearly stretched by NDVI = DN × 0.004 − 0.1, which converts the data range to [0, 1]. The NDVI values of the 20 selected metrological stations were calculated by averaging the values of their eight neighboring pixels, respectively.

Methodology

Three steps were taken to evaluate different temporal characteristics of NDVI and its response to the regional climate variables. Firstly, a wavelet transform was used to reveal the periodicity and nonlinear pattern in changes of NDVI, including wavelet decomposition and reconstruction to approximate the total NDVI over the entire study period at varying time scales. Secondly, correlation analysis was employed to reveal the correlation between NDVI and climate variables, and the change cycle of the NDVI and climate factors were extracted from the wavelet variance at the 20 selected meteorological stations. Lastly, wavelet regression analysis (Xu and others 2008) was applied to reveal the quantitative relationship between NDVI and climate variables at the most suitable time scale.

Wavelet Analysis

WT has been shown to be a powerful multi-resolution analytical technique for the study of multi-scale and non-stationary processes over finite spatial and temporal domains (Partal 2010; Xu and others 2010a). Basically, the idea of WT is the decomposition of a signal at different spatial or time scales onto a set of basis functions (Gabor 1946). In other words, WT uses local basis functions (wavelets) that can be stretched and translated with a flexible resolution in both frequency and time domains to analyze signals. It can be understood as a technique that looks at different sections of the time series with a window adjusted by changing its size, so that a narrow window captures the presence of short-lived events (high frequency variability), whereas a wide window resolves processes that show low frequency variability in time scale.

Formally, a continuous wavelet function that depends on a non-dimensional time parameter η can be written as (Labat 2005):

$$\psi(\eta) = \psi(a,b) = |a|^{-1/2}\psi\left(\frac{t-b}{a}\right) \tag{1}$$

Where t is time, a is the scale parameter and b is the translation parameter. The continuous wavelet transform (CWT) of a discrete signal $x(t)$, such as the time series of NDVI, runoff, temperature, or precipitation, is expressed by the convolution of $x(t)$ with a scaled and translated $\Psi(\eta)$,

$$W_x(a,b) = |a|^{-1/2}\int_{-\infty}^{+\infty} x(t)\Psi^*\left(\frac{t-b}{a}\right)\mathrm{d}t \tag{2}$$

where (*) is the complex conjugate, and $W_x(a,b)$ is the wavelet coefficient. Thus, the concept of frequency is replaced by that of scale, which can characterize the variation in the signal $x(t)$ at a given time scale.

For different combinations of scale a and location b resulting in the decomposition of the signal into time-scale space, a series of wavelet coefficients can be obtained for these specific points. The wavelet coefficients can be interpreted as proportional to the differences between temporally adjacent averages of portions of a time series. This physical interpretation has rendered the WT useful for evaluating how stable such averages are over time. The wavelet variance means the integral of the squared wavelet coefficient to b in the time domain, which can be expressed as:

$$W_x(a) = \int_{-\infty}^{+\infty} |W_x(a,b)|^2\mathrm{d}b \tag{3}$$

From the definition, wavelet variance is a function of scale. It reflects the energy distribution with scale, with high values at a given scale reflecting either the presence of a greater number of peaks or a greater intensity of the signal, or both. The wavelet variance is usually used to detect the periods present in the signal $x(t)$.

By decomposition on the basis of the discrete wavelet transform (DWT), the nonlinear pattern of a time series $x(t)$ can be analyzed at multiple scales. The DWT is defined taking discrete values of a and b. The full DWT for signal $x(t)$, can be represented as (Mallat 1989):

$$x(t) = \sum_k \mu_{j_0,k}(t) + \sum_{j=1}^{j_0}\sum_k \omega_{j,k}\Psi_{j,k}(t) \tag{4}$$

where $\varphi_{j0,k}(t)$ and $\Psi_{j,k}(t)$ are the flexing and parallel shift of the basic scaling function, $\varphi(t)$, and the mother wavelet function, $\Psi(t)$, and $\mu_{j0,k}$ $(j < j_0)$ and $\omega_{j,k}$ are the scaling coefficients and the wavelet coefficients, respectively.

We can represent the approximation in a more revealing manner:

$$x(t) = S_{j_0} + D_{j_0} + D_{j_0-1} + \cdots + D_j + \cdots + D_1 \quad (5)$$

Where

$$S_{j_0} = \sum_k \mu_{j_0,k} \emptyset_{j_0,k}(t)$$

and

$$D_j = \sum_k \omega_{j,k} \psi_{j,k}(t), j = 1, 2, \ldots j_0$$

In general, we have

$$S_{j-1} = S_j + D_j \quad (6)$$

where $\{S_{j_0}, S_{j_0-1}, \ldots S_1\}$ is a sequence of multi-resolution approximations of the function $x(t)$ at ever-increasing levels of refinement.

Based on a selected mother wavelet, the MRA can be conducted. A signal can be used to decompose according to time scale using WT, allowing separation of the fine-scale behavior (detail) from the coarse-scale behavior (approximation) of the signal (Bruce and others 2002). Usually, the fine scale corresponds to a compressed wavelet as well as rapidly changing details (high frequency), whereas coarse scale corresponds to a stretched wavelet and slowly changing coarse features (low frequency). Signal decomposition is typically conducted in an iterative fashion using a series of scales as $J = 2^j$ ($j = 1, 2, \ldots, j_0$, j_0 is the maximum scale sustainable by the number of data points), with successive approximations being split in turn so that one signal is broken down into many lower resolution components (Xu and others 2010b).

It is a prerequisite to select a proper wavelet function for time series analysis (Xu and others 2004). The actual criteria for wavelet selection include self-similarity, compactness, and smoothness. For the present study, Symmlet was chosen as the base wavelet according to these criteria. Using this base wavelet, a number of scaling functions were experimented to determine the most suitable wavelet for these datasets of NDVI and climate factors. It was found that 'Sym8' produced the most robust quantitative results. Therefore, 'Sym8' was chosen as the base wavelet in this paper.

One major interest of this research is to obtain the approximate components based on wavelet decomposition for the time series of NDVI. To accomplish that, the maximum scale analyzed were restricted to $j_0 = 5$. These five time scales are designated as S1 through S5 and started from 20-day (S1), then increased by twofold for the next scale level until a 320-day time scale was attained (S5). Therefore, the levels analyzed were restricted to S1, S2, S3, S4, and S5 to represent the approximate components.

Correlation Analysis

Correlation analysis is a standard statistical measurement of the systematic relationship between two variables. It is calculated for variables x and y as:

$$r_{xy} = \frac{\sum_{j=1}^{n} (x_i - \bar{x})(y_i - \bar{y})}{\sqrt{\sum_{i=1}^{n} (x_i - \bar{x})^2} \sqrt{\sum_{i=1}^{n} (y_i - \bar{y})^2}} \quad (7)$$

where n is the sample number; x_i represents the value of x for the sample i; y_i represents the value of y for the sample i; $\bar{x}$ is the mean for all x_i; $\bar{y}$ is the mean for all y_i. Testing for the significance of the correlation coefficient commonly employs the t distribution.

In this study, correlation analysis was used to check the strength of relations between NDVI and the related climate factors, i.e. temperature, precipitation, relative humidity, and sunshine hours.

Wavelet Regression Analysis

Both NDVI time series and the climate factors time series were usually non-stationary, presenting different components with different frequencies, such as seasonal variations, long-term and short-term fluctuations. It might therefore be difficult to establish a quantitative relationship between NDVI and climate factors as it was commonly done in many other studies. To understand the response of NDVI to regional climate factors during the 11-year period and find the most suitable time scale for investigating the response of NDVI to climate factors, a wavelet regression analysis (Xu and others 2008, 2011) was employed to examine the response of NDVI to climate factors. The basic ideas were as follows: based on the results from wavelet approximation, the statistical relationship between NDVI and the related climate factors were established at a range of time scales using regression analyses; then, the most significant regression models and the time scales most suitable for investigating the response of NDVI to climate factors were identified.

Results

Fluctuation Patterns of NDVI

Using WT, nonlinear patterns of NDVI during the study period were analyzed. Firstly, CWT was adopted to identify the NDVI change cycle. Secondly, the nonlinear

Table 1 The local maximum value of wavelet variances for NDVI, precipitation, temperature, relative humidity, and sunshine hours at the 20 stations (unit: 10-day)

No.	Station	NDVI	Precipitation	Relative humidity	Temperature	Sunshine hours	Vegetation types
1	Jurh	29	29	35	29	29	Desert steppe
2	East Ujimqin Banner	29	29	36	29	28	Typical steppe
3	Abag Banner	28	29	33	29	28	Typical steppe
4	West Ujimqin Banner	29	29	16	29	29	Typical steppe
5	Jarud Banner	29	28	30	29	28	Typical steppe
6	Xilinhot	29	30	33	29	29	Typical steppe
7	Linxi	29	28	31	29	29	Typical steppe
8	Tongliao	28	29	30	29	28	Typical steppe
9	Chifeng	29	28	30	29	30	Typical steppe
10	Qianguoerluosi	28	29	32	29	29	Meadow steppe
11	Harbin	28	28	17	29	29	Meadow steppe
12	Bairin Left Banner	28	28	30	29	29	Meadow steppe
13	Changchun	28	29	33	29	29	Meadow steppe
14	Duolun	28	29	35	29	30	Meadow steppe
15	Tonghe	29	29	181	29	31	Forest
16	Shangzhi	29	29	184	29	29	Forest
17	Mudanjiang	29	28	36	29	30	Forest
18	Siping	28	28	32	29	178	Forest
19	Zhangwu	28	28	30	28	28	Forest
20	Yanji	29	28	30	29	30	Forest

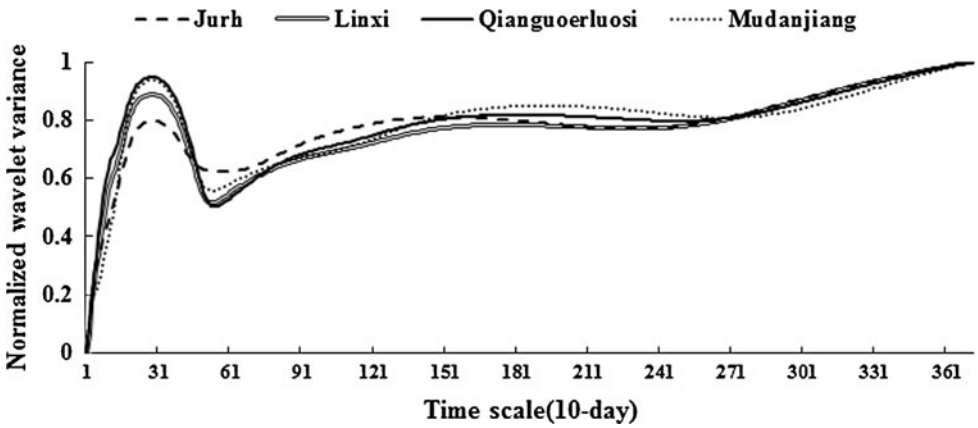

Fig. 2 Normalized wavelet variances of the NDVI at the four selected stations

pattern of NDVI at varying time scale was diagnosed based on DWT.

Periodicity of NDVI

Based on the wavelet function of sym8, the CWT was applied to the NDVI time series of 20 meteorological stations along the NECT. The normalized wavelet variances for the 20 meteorological stations were computed, and their local maximal values (Table 1) were derived. In the example of the four case stations (Fig. 2), the local maxima of wavelet variance for three stations (i.e., Jurh, Linxi and Mudanjiang, which take desert steppe, typical steppe and forest as their vegetation types, respectively) occurred on the 29th 10-day point, whereas this value occurred on the 28th 10-day point for the Qianguoerluosi station in meadow steppe. The results imply that NDVI had a 290-day cycle for Jurh, Linxi and Mudanjiang station and a 280-day cycle for Qianguoerluosi station over the study period.

As shown in Table 1, the NDVI series at the 20 stations showed the cyclic period of either 280-day or 290-day. For different vegetation types, the periodicities of NDVI were of little difference over the study period.

The wavelet coefficients (Fig. 3) of the transect's NDVI time series revealed the existence of 290- or 280-day periodicity in vegetation coverage dynamics. There were two breakpoints every year, May (April for some years) and November, separating the high vegetation coverage period from the low period. Specifically, the wavelet coefficients for the period of May (April for some years) to November were all greater than zero, indicating a high NDVI season.

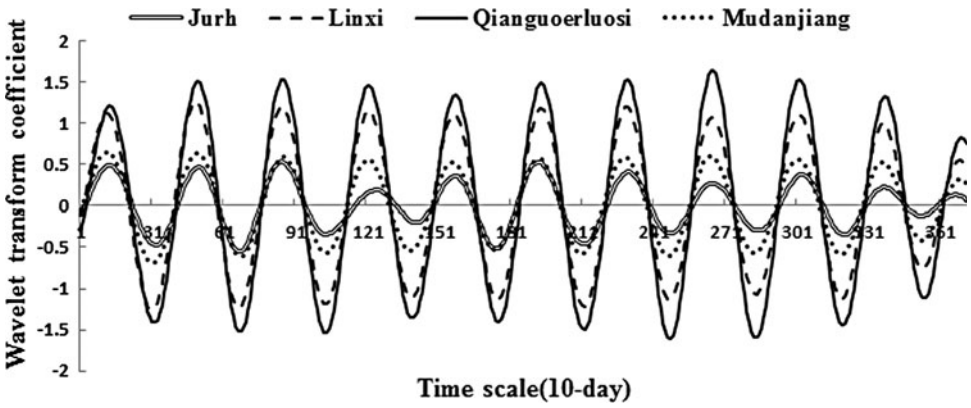

Fig. 3 Wavelet coefficients of NDVI time series

However, the wavelet coefficients of November to May (April for some years) were less than zero, implying it being the low NDVI season. The peak of the wavelet coefficient appeared in August, and the valley in February.

Fluctuation Patterns of NDVI Depending on the Time-Scale

Based on the SPOT-VGT images, the original NDVI time series for 20 meteorological stations were built. These series all showed a fluctuating characteristic. As shown in the Mudanjiang station (Fig. 4a), the original NDVI time series showed fluctuating patterns of NDVI for the period of 1998–2008. It is difficult to identify any trend of NDVI change. With the ascending time scale from S1 to S5, the approximate components based on DWT were obtained (Fig. 4b–d). According to this, the nonlinear patterns for NDVI changes were analyzed at multiple-time scales.

The wavelet decomposition for the time series of NDVI at five time scales resulted in five variants of nonlinear patterns (Fig. 4b–d). The S1 curve (Fig. 4b) is smoother than the original signal but still retains a large amount of residual noise from the raw data. It shows 11 peaks and 10 valleys while each peak and valley has multiple sub-peaks and sub-valleys. These characteristics indicate that although the NDVI varied greatly throughout the study period, there was a hidden trend. At the 40-day scale, the S2 curve (Fig. 4c) still retains a considerable amount of residual noise. However, it is much smoother than the S1 curve, which allows the hidden trend to be more apparent. Compared to S2, the S3 curve (Fig. 4d) retains much less residual noise, and presents obvious periodicity, which is indicated by the 11 peaks without sub-peak and 10 valleys with fewer sub-valleys. Perceptibly, this pattern is more obvious in the S4 curve (Fig. 4d) at the time scale of 160-day than that in the S3 curve. Finally, the S5 curve (Fig. 4d) at the time scale of 320-day, nearly 1 year, presents a clear stable pattern. Therefore, the nonlinear patterns of NDVI were found to be dependent on the time scale.

The Response of NDVI to Climate Factors

Correlations Between NDVI and the Relevant Climate Factors

A correlation analysis between NDVI and the climate factors in NECT was performed based on the times series of 372 data points on NDVI, precipitation, temperature, relative humidity and sunshine hours at the 20 meteorological stations. The results (Table 2) indicate that NDVI exhibited a significant and positive correlation with precipitation, temperature and sunshine hours, but a negative correlation with relative humidity at some sites. The relation between NDVI and temperature was the highest, followed by precipitation, sunshine hours and relative humidity. On the other hand, different vegetation types also showed different strengths in correlation between NDVI and the climate variables. Overall, the correlation coefficients between NDVI and precipitation and temperature increased from desert steppe to typical steppe, meadow steppe, and forest.

Similarity of Periodicity Between NDVI and the Climate Factors

Although the high values of correlation coefficients have no doubt revealed the existence of climatic impact on the NDVI dynamics in NECT, it is still instrumental to investigate the morphological similarity between both temporal patterns. To accomplish that, normalized wavelet variances (Fig. 5) of four climate factors (i.e., precipitation, temperature, relative humidity, and sunshine hours) for the 20 selected meteorological stations were computed, and their local maximal values (Table 1) were derived. In the example of the Mudanjiang station (Fig. 5), the local maxima of wavelet variance for the above climate factors occurred on the 28th, 29th, 36th, and 30th 10-day points, respectively. These temporal points could be regarded as cyclic points for these factors. As illustrated in Fig. 5, the cycles of precipitation and temperature approximated those of NDVI, i.e. 290 days.

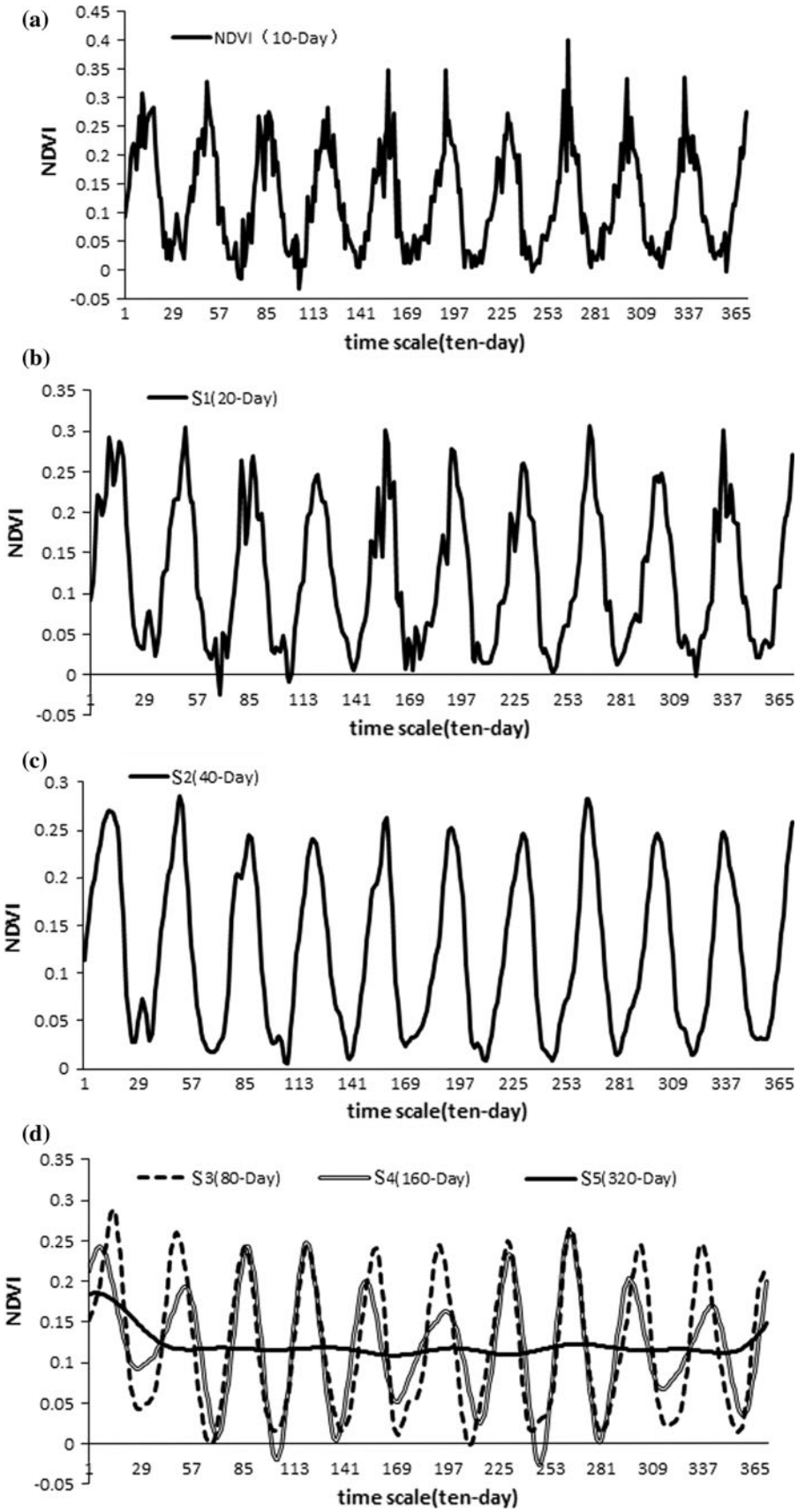

Fig. 4 Nonlinear patterns for NDVI at different time scales

Table 2 The correlation coefficients between NDVI and climate factors

No.	Station	NDVI vs. P	NDVI vs. T	NDVI vs. H	NDVI vs. S	Vegetation types
1	Jurh	0.453**	0.669**	−0.016	0.382**	Desert steppe
2	East Ujimqin Banner	0.456**	0.739**	−0.128*	0.471**	Typical steppe
3	Abag Banner	0.476**	0.793**	−0.3**	0.50**	Typical steppe
4	West Ujimqin Banner	0.494**	0.826**	−0.097	0.505**	Typical steppe
5	Jarud Banner	0.361**	0.738**	0.612**	0.143**	Typical steppe
6	Xilinhot	0.454**	0.81**	−0.25**	0.493**	Typical steppe
7	Linxi	0.485**	0.805**	0.562**	0.389**	Typical steppe
8	Tongliao	0.446**	0.791**	0.536**	0.212**	Typical steppe
9	Chifeng	0.487**	0.757**	0.613**	0.386**	Typical steppe
10	Qianguoerluosi	0.497**	0.803**	0.49**	0.373**	Meadow steppe
11	Harbin	0.497**	0.79**	0.28**	0.446**	Meadow steppe
12	Bairin Left Banner	0.436**	0.79**	0.569**	0.38**	Meadow steppe
13	Changchun	0.533**	0.846**	0.311**	0.335**	Meadow steppe
14	Duolun	0.554**	0.874**	0.227**	0.245**	Meadow steppe
15	Tonghe	0.542**	0.835**	0.238**	0.312**	Forest
16	Shangzhi	0.576**	0.826**	0.375**	0.353**	Forest
17	Mudanjiang	0.514**	0.846**	0.287**	0.396**	Forest
18	Siping	0.541**	0.8**	0.433**	0.055	Forest
19	Zhangwu	0.467**	0.719**	0.633**	0.204**	Forest
20	Yanji	0.485**	0.891**	0.665**	0.236**	Forest

P precipitation, *T* temperature, *H* relative humidity, *S* sunshine hours

* Correlation is significant at the 0.05 level (2-tailed)

** Correlation is significant at the 0.01 level (2-tailed)

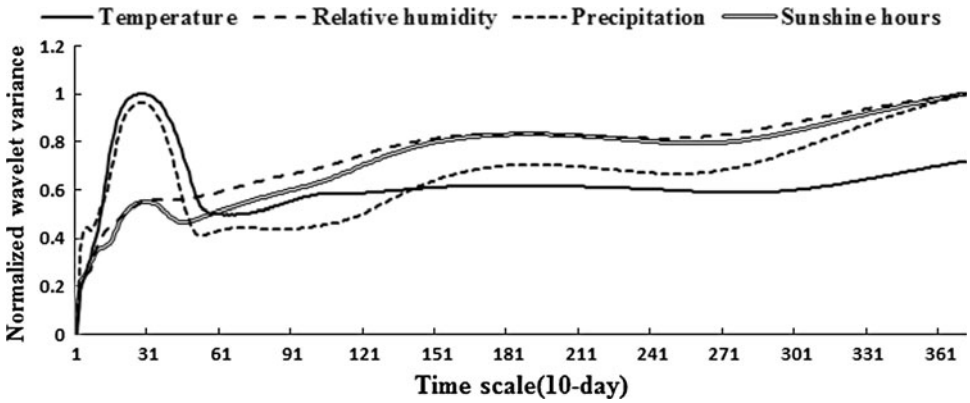

Fig. 5 Normalized wavelet variances of the climate factors at the Mudanjiang station

Similar observations were also obtained from Table 1. Hereby the precipitation and temperature also had either 280- or 290-day change cycle across all 20 stations. Specifically, five stations (i.e., East Ujimqin Banner, West Ujimqin Banner, Tonghe and Shangzhi) had the same 290-day cycle for both NDVI and the two climate factors, while one station (i.e., Zhangwu) had the same 280-day cycle for both. The remaining 14 stations exhibited their climatic cycles 10 days either earlier or later than the NDVI cycle. Nevertheless, the temporal similarities between NDVI and climatic cycles were considerably high. This observation from a new perspective further supported the earlier findings about the close relationship between NDVI and its climate factors.

The Quantitative Relation Between NDVI and the Related Climate Factors

Based on the close NDVI-climate factors correlation revealed in the aforementioned studies, further investigations became necessary to interpret the vegetation dynamic responses to the changes in climate variables and establish quantitative relations between them. This was done through

Table 3 The regression equations between NDVI and climate factors at different time scales for the Duolun station

Time scale	Regression equation	R^2	F	Significance level a
S1	$N = 0.71T + 0.45P - 0.12$	0.81	810.09	0.001
S2	$N = 0.6T + 0.53P - 0.04$	0.85	1055.94	0.001
S3	$N = 0.49T + 0.57P - 0.05$	0.89	1486.54	0.001
S4	$N = 0.45T + 0.48P + 0.02$	0.9	1718.04	0.001
S5	$N = 0.65T + 0.31P + 0.11$	0.44	143.29	0.001

N 10-day maximum NDVI, *P* 10-day average precipitation, *T* 10-day average temperature, *S1* 20-day, *S2* 40-day, *S3* 80-day, *S4* 160-day, *S5* 320-day

the following three steps. Firstly, nonlinear patterns of NDVI and relevant climate factors were approximated at ascending time scales. Secondly, the statistical relationship between NDVI and the related climate factors were established at given time scales through regression analyses of the results from wavelet approximation. Finally, the most significant regression models and the most suitable time scales for investigating the NDVI response to climate changes were identified.

The analytical results (Table 3) indicated that each regression model is statistically significant at the 0.001 level. All the regression models yielded meaningful explanations in which NDVI is positively correlated with temperature and precipitation at all the time scales under examination (i.e. 20-day, 40-day, 80-day, 160-day, and 320-day). Furthermore, the regression models at 20-day, 40-day, and 320-day scales revealed a stronger relationship between NDVI and temperature, while models at 80-day and 160-day scales revealed a stronger relationship between NDVI and precipitation. These results provided further evidence supporting the view that the nonlinear pattern of NDVI is influenced by regional climate variables. In addition, the regression model at S4 scale (i.e.160-day) was found to be the most significant. As a result, the 160-day could be regarded as the most suitable time scale for evaluating the response of vegetation dynamics to climate factors at the Duolun station.

For the other stations, the same analytic steps were taken. The regression models at the most suitable time scales for evaluating the response of NDVI to climate factors were produced (Table 4). For most stations, the most suitable scale was S4 (i.e. 160-day), except the Tonghe station and Jurh station where it was S5 (320-day) and S3 (80-day) respectively. In addition, the regression coefficient indicated that the correlations between NDVI and precipitation were decreasing from desert steppe to typical steppe, meadow steppe, and forest, whereas, the correlations between NDVI and temperature increased gradually along the same order of cover types.

The above results suggested that although the time series of NDVI, temperature, and precipitation presented nonlinear pattern, NDVI had a linear correlation with the temperature and precipitation.

Discussion

NDVI Periodicity

The quantity of heat is uniform in NECT, as the transect situated along the latitude line of 43.5°N between 112°E and 130.5°E. This indicated that the phenology of different vegetation varies little within the transect. For different vegetation types, the NDVI time series presented a similar cyclic pattern over the entire 11-year study period, which confirmed the similar phenological period of different vegetation types within the transect. According to the research of Gong and Chen (2009) and Guo and others (2010), the beginning dates of growth for different vegetation in the northeast region of China were at the end of April or in early May, and the ending dates were in late October. The periodical change of NDVI during the study period reflected the change rule of vegetation phenology to a certain degree, i.e., May (April for some years) to November presented high vegetation coverage, and November to May (April for some years) presented low vegetation coverage.

The Response of Vegetation to Climate Factors

Many studies have proved the existence of strong relationships between vegetation change and climate variability, but few could take the periodicity into consideration and investigate the cyclic patterns of NDVI and major climate factors. The present study indicated that the periodicity of NDVI was similar to that of temperature and precipitation in NECT, which has given new insight into the mechanism of vegetation dynamic response to climate change.

NECT demonstrates a large precipitation/moisture gradient, but NDVI presented a stronger relation with temperature than with precipitation. This implied that temperature has a decisive role on vegetation phenology, whereas precipitation plays an overwhelming role on vegetation distribution along the transect.

In the evaluation of the NDVI response to climate factors at the most suitable time scales, the correlations between NDVI and precipitation were found to descend from desert steppe to typical steppe, meadow steppe, and forest. This seemed to confirm the view that precipitation was the decisive factor for vegetation growth in arid and

Table 4 The regression models between NDVI and climate factors at the most suitable time scales

Station	Regression equation	R^2	F	Significance level a	Most suitable scale
Jurh	$N = 0.1T + 0.81P + 0.08$	0.67	369.98	0.001	S3
East Ujimqin Banner	$N = 0.34T + 0.6P + 0.09$	0.76	588.51	0.001	S4
Abag Banner	$N = 0.37T + 0.68P + 0.03$	0.83	919.98	0.001	S4
WestUjimqin Banner	$N = 0.47T + 0.52P + 0.09$	0.88	1387.12	0.001	S4
Jarud Banner	$N = 0.57T + 0.21P + 0.15$	0.71	455.3	0.001	S4
Xilinhot	$N = 0.54T + 0.42P + 0.07$	0.83	921.12	0.001	S4
Linxi	$N = 0.46T + 0.42P + 0.07$	0.81	769.76	0.001	S4
Tongliao	$N = 0.49T + 0.43P - 0.007$	0.78	638.32	0.001	S4
Chifeng	$N = 0.35T + 0.45P + 0.009$	0.71	458.25	0.001	S4
Qianguoerluosi	$N = 0.82T + 0.04P + 0.07$	0.83	922.91	0.001	S4
Harbin	$N = 0.6T + 0.25P + 0.06$	0.79	684.35	0.001	S4
Bairin Left Banner	$N = 0.57T + 0.33P + 0.008$	0.71	457.78	0.001	S4
Changchun	$N = 0.59T + 0.34P + 0.075$	0.83	923.92	0.001	S4
Duolun	$N = 0.45T + 0.48P + 0.018$	0.9	1718.03	0.001	S4
Tonghe	$N = 0.76T + 0.24P - 0.0001$	0.92	1997.32	0.001	S5
Shangzhi	$N = 0.48T + 0.44P + 0.052$	0.85	1068.82	0.001	S4
Mudanjiang	$N = 0.79T + 0.17P + 0.003$	0.86	1099.97	0.001	S4
Siping	$N = 0.54T + 0.38P + 0.097$	0.81	778.56	0.001	S4
Zhangwu	$N = 0.59T + 0.22P + 0.089$	0.73	489.05	0.001	S4
Yanji	$N = 0.81T + 0.09P + 0.044$	0.88	1366.8	0.001	S4

N 10-day maximum NDVI, *P* 10-day average precipitation, *T* 10-day average temperature, *S3* 80-day, *S4* 160-day, *S5* 320-day

semi-arid regions. At the 10-day time scale, however, the correlation coefficients between NDVI and precipitation exhibited an opposite order. The contrasted results indicated that the NDVI response to climate factors was scale-dependent in the temporal dimension. The coarse time scales usually omit the slight details, and the fine scale generally cannot present the trends.

The NECT starts from Erenhot, Inner Mongolian (IM) in the west, and extends from Inner Mongolian Plateau in the west and Liaohe River alluvial plain in the middle to north Changbai Mountain in the east. Yang and others (2012) employed a similar method to study the vegetation dynamic and its response to climate factors in IM. Geographically, the study areas partially overlapped. Some similar conclusions were obtained such as the cyclic period of NDVI and temperature and precipitation. But many differences from the data processing method to conclusions were found when the integrated method was applied to the transect. First, for the greater representation of the selected metrological stations, the NDVI values of the metrological stations were obtained by averaging the values from eight neighborhoods in this study, instead of simply taking the coordinates like the study of IM. Based on this, the periodicity of NDVI for some stations was not same, such as Abag Banner, Jarud Banner, and Bairin Left Banner station. They were 10 days later or earlier than the NDVI periodicity between the same stations. The same difference was found in the correlation between NDVI and climate factors, i.e., the correlation coefficients at the same stations were not completely the same. At last, the biggest difference was the most suitable time scales for evaluating the response of NDVI to climate factors. It is 160 days for most stations in this study, and 80 days in the study of IM.

Due to the complexity of vegetation dynamic and regional climate factors change coupled with the impact of human activity, it is difficult to understand how the coupling of vegetation dynamic and climate factors change. The methods used in the study were still statistical in nature, lacking an investigation of the mechanism. Therefore, further studies with better methods and results will be expected.

Conclusions

This study investigated the vegetation dynamics of the NECT by coupling SPOT-VGT image-based NDVI time series (1988–2008) with the climate data from 20 meteorological stations within the study area. The investigation was conducted using three methods, with each looking into one aspect of the issue. A WT was first applied to detect and diagnose the periodicity and nonlinear patterns of NDVI time series. Correlation analyses between NDVI and

climate time-series data were then conducted, and the WT was used again to reveal the change cycles of relevant climate factors. At last, wavelet regression analyses were used to quantify the relationships between NDVI and climate factors at a range of time scales and to identify the time scales most suitable for evaluating the impact of climate factors on NDVI at the 20 stations.

The analytical results from above efforts led to following significant findings.

1. A cyclic period of either 280 or 290 days was detected in the NDVI time series, and there was no noticeable variation in the periodicity of NDVI among vegetation types over the entire 11-year study period. The break of the 280-day (or 290-day in some cases) NDVI cycle fell into either May (April for some years) or November, with May (April for some years)–November being the high NDVI season and November–May (April for some years), the low season, which reflected the change rule of vegetation phenology to a certain degree. In addition, the nonlinear NDVI pattern was found to be scale-dependent in the time domain. The wavelet decomposition of the NDVI time series at the five time scales resulted in five variants of a nonlinear, stable pattern. With the time scale changing from small to large, the wavelet curves became incrementally smoother and stabilizing onto an obvious tendency.
2. There was a close relationship between temporal variations in the NDVI and regional climate factors. The NDVI was found to significantly correlate with precipitation, temperature, and sunshine hours in a positive fashion but negatively correlate with relative humidity at some sites. The relation between NDVI and temperature was the highest, followed by precipitation, sunshine hours, and relative humidity. Different vegetation cover types showed different strengths in correlation between NDVI and the climate variables, and the correlation values increased from desert steppe to typical steppe, meadow steppe, and forest in the whole.
3. Temporal cycles of 280 and 290 days were detected from the precipitation and temperature time series, respectively. The cycles were found to coincide with the cyclic period of the NDVI, suggesting that the relationship between NDVI and its climate factors could be explored from a new perspective.
4. At all the time scales under examination (i.e., 20-, 40-, 80-, 160-, and 320-day), NDVI and the climate factors (i.e. temperature and precipitation) were significantly and positively correlated at the 20 selected stations. The most suitable time scale to investigate the responses of vegetation dynamic to climate factors was 160-day for most stations. At the most suitable time scales, the correlations between NDVI with precipitation were decreasing from desert steppe to typical steppe, meadow steppe, and forest; however, the correlations between NDVI with temperature were increased gradually, confirming the view that precipitation was the decisive factor controlling different vegetation distribution in the study area. The results suggested that although the time series of NDVI, temperature, and precipitation presented nonlinear patterns, NDVI had a linear correlation with the temperature and precipitation.

Acknowledgments This work was supported by National Natural Science Foundation of China (Grant No. 41130525, 41040015). The authors are very grateful to Editors in Chief, Professor Virginia Dale and Rebecca Efroymson, and the anonymous referees for their hard work and generous comments given for the improvement of the manuscript.

References

Asrar G, Fuchs M, Kanemasu ET, Hatfield JL (1984) Estimating absorbed photosynthetic radiation and leaf area index from spectral reflectance in wheat. Agronomy Journal 76:300–306

Bruce LM, Koger CH, Li J (2002) Dimensionality reduction of hyperspectral data using discrete wavelet transform feature extraction. IEEE Transactions on Geoscience and Remote Sensing 40(10):2331–2338

Burke-Hubbard B (1998) The World according to wavelets. The story of a mathematical technique in the making, 2nd edn. A.K. Peters, Natick, p 330

Canadell JG, Steffen WL, White PS (2002) IGBP/GCTE terrestrial transects: dynamics of terrestrial ecosystems under environmental change. Journal of Vegetation Science 13:298–300

Cao L, Xu JH, Chen YN, Li WH, Yang Y, Hong YL, Li Z (2012) Understanding the dynamic coupling between vegetation cover and climatic factors in a semiarid region—a case study of Inner Mongolia, China. Ecohydrology. doi:10.1002/eco.1245

Chen XW, Wang FY (2000) Simulation of the potential responses of the communities of mixed coniferous and broadleaf Korean pine to climatic change by BKPF forest gap model. Acta Phytoecologica Sinica 24:327–331

Chen XW, Zhang XS, Zhou GS, Chen JZ (2000) Spatial characteristics and change for tree species (genera) along Northeast China Transect (NECT). Acta Botonica Sinica 42:1075–1081

Chen XW, Zhou GS, Zhang XS (2003) Spatial characteristics and change for tree species along the North East China Transect (NECT). Plant Ecology 164:65–74

Diodato N, Bellocchi G (2008) Modelling vegetation greenness responses to climate variability in a Mediterranean terrestrial ecosystem. Environmental Monitoring and Assessment 143(1–3):147–159

Fonseca LMG, Costa MHM, Manjunath BS, Kenny C (1998) Automatic registration of satellite imagery. In: Proceedings of "Image Registration Workshop", NASA Goddard Space Flight Center, Greenbelt, pp 13–27

Fu XF, Yang ST, Liu CM (2007) Changes of NDVI and their relations with principal climatic factors in the Yarlungzangbo river basin. Geographical Research 26(1):60–66

Furon AC, Wagner-Riddle C, Smith CR, Warland JS (2008) Wavelet analysis of wintertime and spring thaw CO_2 and N_2O fluxes from

agricultural fields. Agricultural and Forest Meteorology 148: 1305–1317
Gabor D (1946) Theory of communication. Proceedings of the Institute of Electrical Engineers 93(26):429–457
Galford GL, Mustard JF, Melillo J, Gendrin A, Cerri CC, Cerri CEP (2008) Wavelet analysis of MODIS time series to detect expansion and intensification of row-crop agriculture in Brazil. Remote Sensing of Environment 112:576–587
Gao Q, Zhang XS (1997) A simulation study of responses of the Northeast China Transect to elevated CO2 and climate change. Ecological Applications 7:470–483
Garty J, Tamir O, Hassid I, Eshel A, Cohen Y, Karnieli A, Orlovsky L (2001) Photosynthesis, chlorophyll integrity and spectral reflectance in lichens exposed to air pollution. Journal of Environmental Quality 30(3):884–893
Giannico C (2007) Remote sensing of vegetation in the Calabrian region. Acta Astronautica 60:119–131
Gong P, Chen ZX (2009) Regional vegetation phenology monitoring based on MODIS. Chinese Journal of Soil Science 40(2):213–217
Guo ZX, Zhang XN, Wang ZM, Fang WH (2010) Simulation and variation pattern of vegetation phenology in Northeast China based on remote sensing. Chinese Journal of Ecology 29(1):165–172
Hall-Beyer M (2003) Comparison of single-year and multiyear NDVI time series principal components in cold temperate biomes. IEEE Transactions on Geoscience and Remote Sensing 41(11):2568–2574
Horgan G (1998) Wavelets for SAR image smoothing. Photogrametric Engineering and Remote Sensing 64:1171–1177
Jarlan L, Mangiarotti S, Mougin E (2008) Assimilation of SPOT/VEGETATION NDVI data into a Sahelian vegetation dynamics model. Remote Sensing of Environment 112(4):1381–1394
Koch GW, Scholes RJ, Steffen WL, Vitousek PM, Walker BH (1995) The IGBP terrestrial transects: science Plan. International Biosphere–Geosphere Programme (IGBP), Stockholm, p 61
Labat D (2005) Recent advances in wavelet analyses: Part 1. A review of concepts. Journal of Hydrology 314:275–288
Li J, Bruce LM (2004) Wavelet-based feature extraction for improved endmember abundance estimation in linear unmixing of hyperspectral signals. IEEE Transactions on Geoscience and Remote Sensing 42:644–649
Li YC, Chen J, Gong P (2005) Study on land cover change detection method based on NDVI time series datasets: change detection indexes design. Journal of Basic Science and Engineering 13(3): 261–275
Maisongrande P, Duchemin B, Dedieu G (2004) VEGETATION/SPOT: an operational mission for the Earth monitoring; presentation of new standard products. International Journal of Remote Sensing 25(1):9–14
Mallat SG (1989) A theory for multiresolution signal decomposition: the wavelet representation. IEEE Transactions on Pattern Analysis and Machine Intelligence 11(7):674–693
Ni J, Wang GH (2004) Northeast China Transect (NECT): ten-year synthesis and future challenges. Acta Botanica Sinica 46(4): 379–391
Ni J, Zhang XS (2000) Climate variability, ecological gradient and the Northeast China Transect (NECT). Journal of Arid Environments 46:313–325
Ni J, Li YY, Zhang XS (1999) The scientific significance of the Northeast China Transect (NECT) to global change study by its ecogeographic characteristics. Acta Ecologica Sinica 19:622–629
Partal T (2010) Wavelet transform-based analysis of periodicities and trends of Sakarya basin (Turkey) streamflow data. River Research and Application 26(6):695–711
Sakamoto T, Yokozawa M, Toritani H, Shibayama M, Ishitsuka N, Ohno H (2005) A crop phenology detection method using time-series MODIS data. Remote Sensing of Environment 96:366–374
Simhadri KK, Iyengar SS, Holyer RJ, Lybanon M, Zachary JM (1998) Wavelet based feature extraction from oceanographic images. IEEE Transactions on Geoscience and Remote Sensing 36:767–777
Steffen WL (1995) Rapid progress in IGBP Transects. Global Change Newsletter 24:15–16
Steffen WL, Scholes RJ, Valentin C, Zhang X, Menaut JC, Schulze ED (1999) The IGBP terrestrial transects. The terrestrial biosphere and global change. Cambridge University Press, Cambridge, pp 66–87
Stockli R, Vidale PL (2004) European plant phenology and climate as seen in a 20-year AVHRR land-surface parameter dataset. International Journal of Remote Sensing 25(17):3303–3330
Udelhoven T, Stellmes M, del Barrio G, Hill J (2009) Assessment of rainfall and NDVI anomalies in Spain (1989–1999) using distributed lag models. International Journal of Remote Sensing 30(8):1961–1976
Wang RZ, Ripley EA, Zu YG, Nie SQ (2001) Demography of sexual and biomass allocation of grassland and dune *Leymus chinensis*: an analog for response to environment change. Journal of Arid Environments 49:289–299
Xu JH, Lu Y, Su FL, Ai NS (2004) R/S and wavelet analysis on the evolutionary process of regional economic disparity in China during the past 50 years. Chinese Geographical Science 14(3):193–201
Xu JH, Chen YN, Ji MH, Lu F (2008) Climate change and its effects on runoff of Kaidu River, Xinjiang, China: a multiple time-scale analysis. Chinese Geographical Science 18(4):331–339
Xu JH, Li WH, Ji MH, Lu F, Dong S (2010a) A comprehensive approach to characterization of the nonlinearity of runoff in the headwaters of the Tarim River. Western China. Hydrological Process 24(2):136–146
Xu JH, Chen YN, Li WH, Yang Y, Hong YL (2010b) An integrated statistical approach to identify the nonlinear trend of runoff in the Hotan River and its relation with climatic factors. Stochastic Environmental Research and Risk Assessment 25(2):223–233
Xu JH, Chen YN, Lu F, Li WH, Zhang LJ, Yang Y (2011) The nonlinear trend of runoff and its response to climate change in the Aksu River, western China. International Journal of Climatology 31(5):687–695
Yang Y, Xu JH, Hong YL, Lv GH (2012) The dynamic of vegetation coverage and its response to climatic factors in Inner Mongolia, China. Stochastic Environmental Research and Risk Assessment 26(3):357–373
Zhang XS, Gao Q, Yang DA, Zhou GS, Ni J, Wang Q (1997a) A gradient analysis and predict ion on the Northeast China Transect (NECT) for global change study. Acta Botanica Sinica 39:785–799
Zhang XS, Zhou GS, Gao Q, Yang DA, Ni J, Tang HP (1997b) Northeast China Transect (NECT) for global change studies. Frontiers of Earth Science 4:145–151
Zhang XS, Gao Q, Yang DA, Zhou GS, Ni J, Wang Q, Tang HP (1998) A gradient analysis and modeling of the Northeast China Transect (NECT) for global change study. Bulletin of the Chinese Academy of Sciences 12:15–21
Zhang J, Pan XL, Gao ZQ (2006) Estimation of net primary productivity of the oasis-desert ecosystems in arid west China based on RS-based ecological process. Arid Land Geography 29(2):255–261
Zhou J, Civco DL, Silander JA (1998) A wavelet transform method to merge Landsat TM and SPOT panchromatic data. International Journal of Remote Sensing 19:743–757
Zhu C, Yang X (1998) Study of remote sensing image texture analysis and classification using wavelets. International Journal of Remote Sensing 19:3197–3203